IOPscience iopscience.iop.org

Home Search Collections Journals About Contact us My IOPscience

Evidence of collinear ferrimagnetism in (Fe, Tb)B metallic glasses from polarized beam neutron scattering

This article has been downloaded from IOPscience. Please scroll down to see the full text article.

2005 J. Phys.: Condens. Matter 17 3585

(http://iopscience.iop.org/0953-8984/17/23/011)

View the table of contents for this issue, or go to the journal homepage for more

Download details:
IP Address: 129.252.86.83
The article was downloaded on 28/05/2010 at 04:58

Please note that terms and conditions apply.

INSTITUTE OF PHYSICS PUBLISHING JOURNAL OF PHYSICS: CONDENSED MATTER

J. Phys.: Condens. Matter **17** (2005) 3585–3596 doi:10.1088/0953-8984/17/23/011

Evidence of collinear ferrimagnetism in (Fe, Tb)B metallic glasses from polarized beam neutron scattering

N Cowlam[1], M D Hanwell[1], A R Wildes[2] and A G I Jenner[3]

[1] Department of Physics and Astronomy, University of Sheffield, Sheffield S3 7RH, UK
[2] Institut Laue-Langevin, BP 156, 38042 Grenoble Cedex, France
[3] Department of Physics, University of Hull, Hull HU6 7RX, UK

Received 31 March 2005, in final form 5 May 2005
Published 27 May 2005
Online at stacks.iop.org/JPhysCM/17/3585

Abstract

The atomic-scale magnetic structures of two terbium-substituted $(Fe_{0.83-x}Tb_x)B_{0.17}$ metallic glasses have been determined by polarized beam neutron scattering measurements using the IN20 spectrometer at the Institut Laue-Langevin, Grenoble. The four spin-dependent, neutron scattering cross-sections were measured in absolute units for the two glasses. The spin-flip cross-sections $\frac{\partial\sigma^{+-}}{\partial\Omega}$ and $\frac{\partial\sigma^{-+}}{\partial\Omega}$ were found to be small; they were independent of the scattering vector Q, independent of the temperature and were also of the same magnitude as the nuclear incoherent cross-section, within experimental errors. These observations indicate that the magnetic structure in these glasses must be collinear. The non-spin-flip cross-sections were found to have a hitherto unobserved shift of the first peak between the $\frac{\partial\sigma^{++}}{\partial\Omega}$ and $\frac{\partial\sigma^{--}}{\partial\Omega}$ channels. A (collinear) ferrimagnetic state which is consistent with the spin-flip cross-sections is therefore proposed for these glasses. The magnetic moments on the terbium atoms are aligned antiparallel to those on the iron atoms, and the values of both moments reduce to zero by $x = 0.50$ terbium, in agreement with magnetization data. A calculation of the non-spin-flip cross-sections based on this model correctly predicts the shift of the first peaks. This behaviour arises because of the ferrimagnetic correlations between the magnetic moments and the very strong magnetic scattering from the terbium atoms.

1. Introduction

The magnetic ground state of the transition-metal–metalloid (TM–met) metallic glasses (of which $Fe_{0.83}B_{0.17}$ is the prototype), has been the subject of considerable interest since Mizoguchi first presented a review of the compositional dependence of their Curie temperature T_C and their mean magnetic moment $\langle\mu\rangle$ [1]. It is generally accepted that the variation of T_C and $\langle\mu\rangle$ for those glasses based on the elemental ferromagnets (Fe, Ni, Co-met) can be explained with a simple rigid band model (plus charge transfer from the metalloid atoms). Alloying with

 © 2005 IOP Publishing Ltd Printed in the UK

manganese, chromium and vanadium on the other hand, gives a much more rapid reduction in $\langle\mu\rangle$ which has been tentatively associated with larger 'free atom'-like moments which are directed antiparallel to the net magnetization [1]. More recently, the presence of non-collinear ferromagnetism in TM–met glasses [2–4] has introduced another factor which influences the values of $\langle\mu\rangle$ derived from bulk properties such as magnetization. Measurements of T_C and $\langle\mu\rangle$ have also been extended to alloys of transition metals from the second and third rows of the periodic table and complex magnetic phase diagrams have been found. These can include ferromagnetic, spin-glass and re-entrant spin-glass phases [5]. Alloying TM–met glasses with the rare earths is of interest because of the possibility of both antiparallel *and* non-collinear alignments of the magnetic moments, similar to those observed in the amorphous RE–TM_2 alloys, described by the random anisotropy model [6]. (TM, RE)–met glasses are also of technological interest because if their magnetostrictive properties can be sufficiently enhanced, they will have potential applications in devices, since their ribbon geometry reduces eddy current effects at high frequencies [7]. Studies of the variation of the magnetization and Curie temperature T_C in $(Fe_{0.82}B_{0.18})_{1-x}Tb_x$ glasses have been made, for example [8], and these show a compensation point in the magnetization at $x = 0.22$ terbium. The magnetic phase diagram shows a steady fall in T_C with increasing terbium concentration that is apparently accompanied by the growth of a 'random anisotropy phase' below the spin freezing temperature T_f, which has a maximum value of $T_f \approx 150$ K (see figures 1 and 2 of [8]). The search for non-collinear ferromagnetism in this 'random anisotropy phase' was the main motivation for the present measurements.

Note that the type of terbium substitution $(Fe_{0.82}B_{0.18})_{1-x}Tb_x$ used in [8] gives a slightly different stoichiometry from the two $(Fe_{0.83-x}Tb_x)B_{0.17}$ samples used in this study. The present method avoids boron-deficient glasses at large values of x, which may be close to the edge of the glass-forming range ($0.09 < B < 0.28$ for FeB glasses [9]), although, in fact, no evidence of crystalline contamination was found in [8].

2. Sample preparation and experimental method

Spectrographically pure iron, terbium and boron were melted and thoroughly mixed in an argon arc furnace to make several master ingots of ≈10 g of $Fe_{0.78}Tb_{0.05}B_{0.17}$ and $Fe_{0.73}Tb_{0.10}B_{0.17}$ alloys. Each of these was divided into two or three pieces and melt-spun in a helium atmosphere onto a steel wheel. When terbium is added to $Fe_{0.83}B_{0.17}$ the resulting glass becomes increasingly more brittle, so the metallic glass ribbon obtained was in short lengths ≈1 mm wide and ≈25 μm thick. Isotopically enriched boron (which reduces the absorption of thermal neutrons) was not used in this preparation, since the material supplied can sometimes influence the viscosity of the melt. X-ray diffraction scans were made to confirm the glassy state of the ribbon samples.

The neutron experiments were made at the IN20 diffractometer at the Institute Laue-Langevin. This has Heusler alloy crystals as monochromator and analyser and spin-flippers in the incident and scattered beams, so that the four spin-dependent scattering cross-sections ($\frac{\partial\sigma^{++}}{\partial\Omega}$, $\frac{\partial\sigma^{--}}{\partial\Omega}$, $\frac{\partial\sigma^{+-}}{\partial\Omega}$ and $\frac{\partial\sigma^{-+}}{\partial\Omega}$ [10]) can be obtained. Most of the experimental details were identical to those specified in our previous measurements on IN20 [3, 4, 11], except that the (brittle) ribbons, which had masses 3.211 g ($Fe_{0.78}Tb_{0.05}B_{0.17}$) and 1.281 g ($Fe_{0.73}Tb_{0.10}B_{0.17}$), were placed in cylindrical aluminium holders. A vertical magnetic field of 2 T was applied to the samples to saturate the domains and avoid depolarization effects. The two samples were measured at 8 and 300 K, over a range of scattering vectors 1.0 $Å^{-1} < Q < 6.5$ $Å^{-1}$, where $Q = 4\pi \sin\theta/\lambda$. The data analysis was performed using our own programs which have been described in detail elsewhere [4, 12]. Note that it is quite difficult to make *perfect*

Table 1. Values of the mean spin-flip cross-sections $\langle \partial\sigma^{\pm\mp}/\partial\Omega \rangle$ and the slope of a linear trend line through the cross-sections shown in figures 1(a) and 2(a) are given. They show that these cross-sections are equal to $2/3(\partial\sigma_{\mathrm{NSI}}/\partial\Omega)$ and also flat over the measured Q range, to within experimental errors.

Composition	Temperature (K)	Mean value of $\langle \partial\sigma^{\pm\mp}/\partial\Omega \rangle$[a] barns sr^{-1}/atom	Slope of $\langle \partial\sigma^{\pm\mp}/\partial\Omega \rangle v Q$ barns sr^{-1}/atom Å
$Fe_{0.78}Tb_{0.05}B_{0.17}$	300	0.02 ± 0.01	-0.001 ± 0.003
	8	0.03 ± 0.02	-0.002 ± 0.003
$Fe_{0.73}Tb_{0.10}B_{0.17}$	300	-0.02 ± 0.01	-0.003 ± 0.010
	8	-0.02 ± 0.01	-0.000 ± 0.008

[a] $2/3(\partial\sigma_{\mathrm{NSI}}/\partial\Omega) = 6.9 \times 10^{-3}$ barns sr^{-1}/atom.

corrections for the background scattering and the absorption when (as here) the Bragg peaks from the aluminium sample holders are so much more intense than the signals from the samples. However, the Bragg peaks are well localized in Q and do not compromise the broad features of the *diffuse* scattering from the glassy samples, which is derived from this type of measurement.

3. Spin-flip cross-sections

The present polarized beam neutron scattering experiments involve the absolute measurement of four spin-dependent scattering cross-sections. Their application to metallic glasses has been discussed previously [2–4] so only a brief outline will be given here.

In one standard configuration [10] of the IN20 instrument, the y-axis is parallel to the scattering vector Q and the vertical magnetic field lies along the z-axis. If a neutron passes through the sample and the direction of its spin is changed because of interactions with the magnetic spins S, then the spin-flip cross-sections $\frac{\partial\sigma^{+-}}{\partial\Omega}$ and $\frac{\partial\sigma^{-+}}{\partial\Omega}$ are identical and are given by [10]

$$\frac{\partial\sigma^{\pm\mp}}{\partial\Omega} = \frac{2}{3}\frac{\partial\sigma_{\mathrm{NSI}}}{\partial\Omega} + \left| \left\langle \sum_{ij} (d_i S_{xi} d_j^* S_{xj}^*) \exp(\mathrm{i}Q(r_i - r_j)) \right\rangle \right|. \tag{1}$$

Here $\frac{2}{3}\frac{\partial\sigma_{\mathrm{NSI}}}{\partial\Omega}$ is the nuclear spin incoherent cross-section which has the value 6.9×10^{-3} barns sr^{-1}/atom for both samples, because it is dominated by their boron content [13]. In the second term, $d_i S_i$ is the magnetic scattering amplitude of the ith atom which carries a spin S_i and in particular depends on only the *non-collinear components* S_x of the magnetic spins. The parameter $d_i = (\gamma e^2/2mc^2) g_i f_i(Q)$ contains the magnetic form factor $f_i(Q)$. The second term in equation (1) arises exclusively from neutron magnetic scattering. This means that if the spin-flip cross-sections are larger than $\frac{2}{3}\frac{\partial\sigma_{\mathrm{NSI}}}{\partial\Omega}$, this provides direct evidence of non-collinear S_x components of the magnetic spins. Conversely, if they have the same magnitude as $\frac{2}{3}\frac{\partial\sigma_{\mathrm{NSI}}}{\partial\Omega}$, then the non-collinear S_x components of the magnetic spins must be zero and the magnetic structure is a conventional, collinear ferromagnet. A finite spin-flip cross-section can, of course, be analysed to provide information on the spatial variation of the S_x components of the spins. In an asperomagnet [6] or a random cone structure [3], for example, the S_x components of the spins point in random directions and there are no spatial correlations between them. The second term in equation (1) then reduces to $\langle d^2 S_x^2 \rangle$ and the spin-flip cross-section follows a form-factor dependence $\langle f(Q)^2 \rangle$.

The average of the $\frac{\partial\sigma^{+-}}{\partial\Omega}$ and $\frac{\partial\sigma^{-+}}{\partial\Omega}$ spin-flip cross-sections measured for the $Fe_{0.78}Tb_{0.05}B_{0.17}$ sample at 8 and 300 K are shown in figure 1(a) and those for the $Fe_{0.73}Tb_{0.10}B_{0.17}$ sample in figure 2(a). The error bars are greater in figure 2(a) because of the smaller mass of the sample. Both these cross-sections are extremely small (see table 1), and probably close to the lower

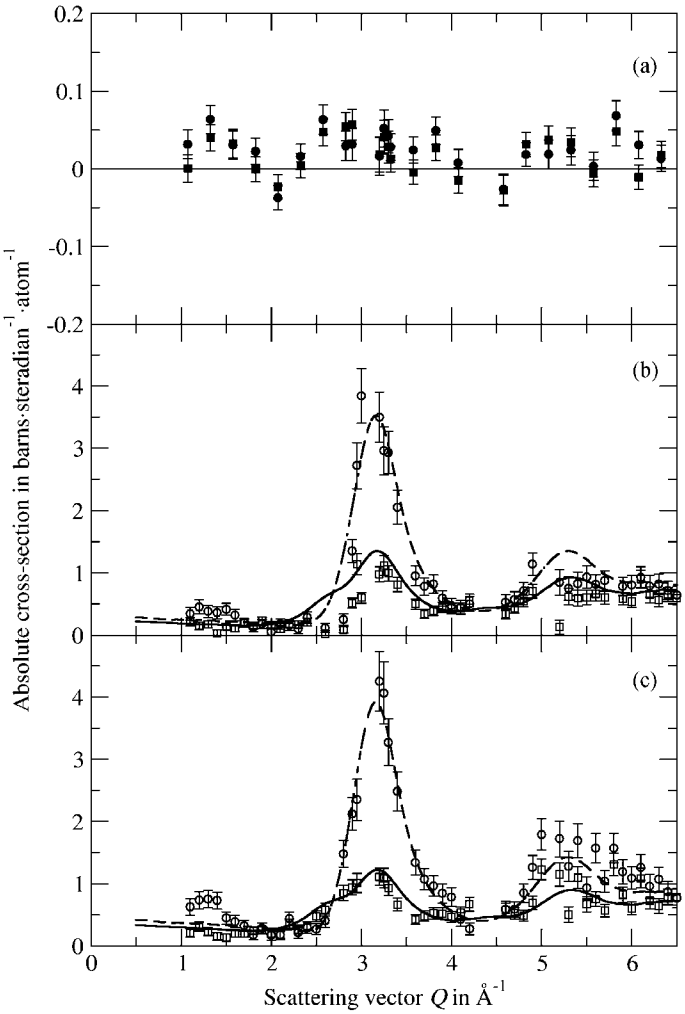

Figure 1. The average spin-flip cross-sections $\langle \partial\sigma^{\pm\mp}/\partial\Omega \rangle$ measured for the $Fe_{0.78}Tb_{0.05}B_{0.17}$ sample at 300 K (■) and at 8 K (●) are shown in (a) and the non-spin-flip cross-sections $\partial\sigma^{--}/\partial\Omega$ (○) and $\partial\sigma^{++}/\partial\Omega$ (□) measured at 300 and at 8 K over the same Q range are shown in (b) and (c), respectively. Note the change of scale (10×) on the ordinate between (a) and (b)/(c).

limit of what can be measured with such samples in this type of experiment. They are also equal, within the experimental errors, to the nuclear spin incoherent term. All this suggests that the magnetic structures in these samples are collinear. In addition, trend lines fitted to these cross-sections show that all four sets of data are flat and that their slopes are zero, to within the experimental errors; see table 1. This rules out the presence of a random cone and asperomagnetic structures which would give form-factor-dependent cross-sections. Finally, the spin-flip cross-sections measured at both 8 and 300 K are superimposed in figures 1(a) and 2(a) (using different symbols), and they are statistically identical. This also rules out any significant magnetic contribution to these cross-sections, which would otherwise vary by about 40% between 8 and 300 K as the aligned components of the magnetic moments vary with temperature (see below).

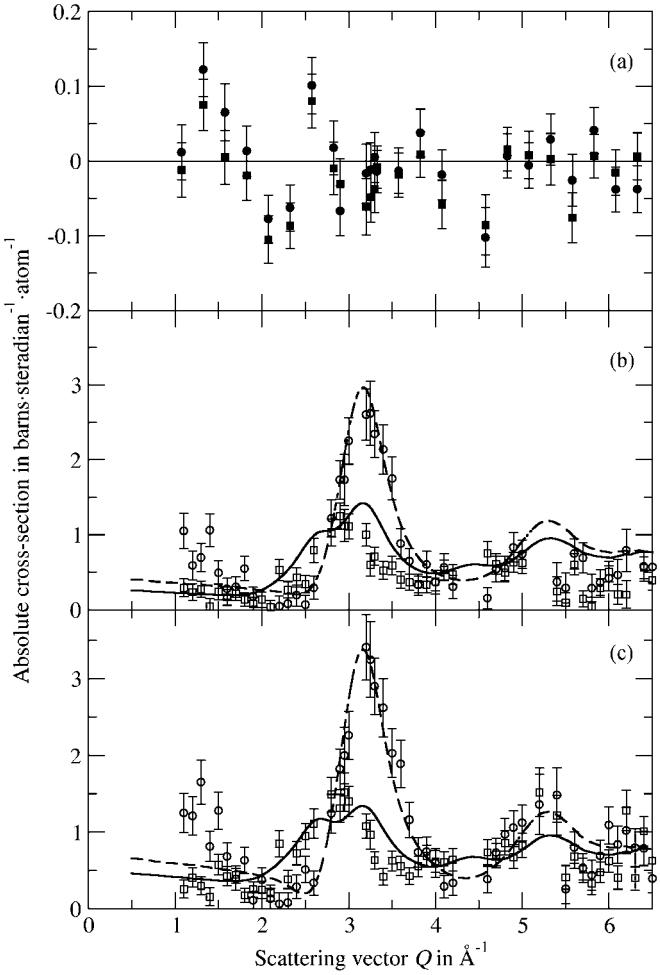

Figure 2. The average spin-flip cross-sections $\langle \partial\sigma^{\pm\mp}/\partial\Omega \rangle$ measured for the $Fe_{0.73}Tb_{0.10}B_{0.17}$ sample at 300 K (■) and at 8 K (●) are shown in (a) and the non-spin-flip cross-sections $\partial\sigma^{--}/\partial\Omega$ (○) and $\partial\sigma^{++}/\partial\Omega$ (□) measured at 300 and at 8 K over the same Q range are shown in (b) and (c) respectively. This shift of the first peak between the two non-spin-flip cross-sections is more strongly developed for this 10% terbium sample. The solid and dotted lines in (b) and (c) are a fit to the data based on the structural model described in the text.

4. A collinear ferrimagnetic structure for $(Fe_{0.83-x}Tb_x)B_{0.17}$ glasses

The magnetic phase diagram for the $(Fe_{0.82}B_{0.18})_{1-x}Tb_x$ glasses given in [8] shows the presence of a 'random anisotropy phase' at low temperatures. However, the measured spin-flip cross-sections given in figure 1 suggest that (Fe, Tb)B glasses are more likely to have collinear ferrimagnetic structures. A simple, collinear ferrimagnet with the magnetic moments on the iron and the terbium atoms based on their elemental values will therefore be presented in this section.

Figure 1 of [8] shows the variation of saturation magnetization with composition in a series of $(Fe_{0.82}B_{0.18})_{1-x}Tb_x$ glasses. It falls rapidly with the addition of terbium and reaches zero at the composition $x = 0.50$. This graph can be redrawn by replotting the points for

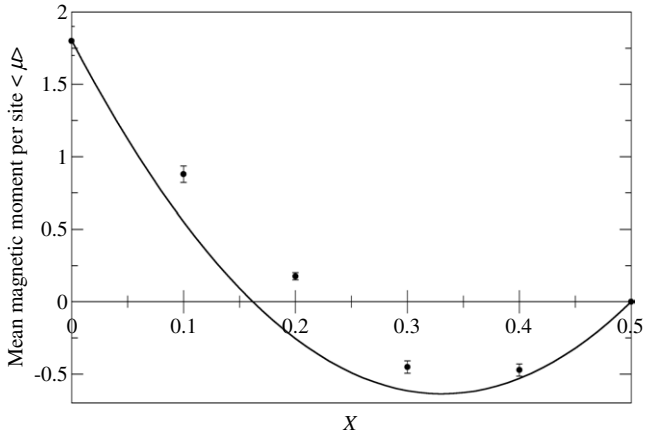

Figure 3. The suggested variation of the mean magnetic moment per site of $\langle\mu\rangle$ for collinear ferromagnetic $(Fe_{0.83-x}Tb_x)B_{0.17}$ glasses is shown by the solid line, together with data points derived from the measured variation of the magnetization presented in figure 1 of [8].

$x = 0.30$ and 0.40 terbium below the abscissa to create the classic graph for a ferrimagnet, which emphasizes the compensation point at $x \approx 0.22$ terbium [8]. In addition, the saturation magnetization of the parent $Fe_{0.82}B_{0.18}$ glass of 1292 kA m^{-1} can be attributed to the saturated moment of 2.2 μ_B on every iron atom [9], so the ordinate can be rescaled to give the mean magnetic moment per site for these glasses $\langle\mu\rangle$. In the simplest case, this value is the difference between an aligned moment of $\mu_{Fe} = 2.2\ \mu_B$ on each iron atom and $\mu_{Tb} = -9.34\ \mu_B$ aligned antiparallel on each terbium atom. The mean magnetic moment per site is then

$$\langle\mu\rangle = (1-2x)[0.82(1-x)\mu_{Fe} - x\mu_{Tb}], \tag{2}$$

where linear reduction $(1-2x)$ allows for the suppression of the ferrimagnetic state at $x = 0.50$. This prediction and the values of $\langle\mu\rangle$ derived from [8] are shown together in figure 3. Whilst the agreement is not perfect, it does at least support the use of this simple model as a working hypothesis. Note that the two glasses from the $(Fe_{0.82}B_{0.18})_{1-x}Tb_x$ series [8], with $x = 0.05$ and 0.10, have ternary compositions of $Fe_{0.779}Tb_{0.05}B_{0.171}$ and $Fe_{0.738}Tb_{0.10}B_{0.162}$ which are sufficiently close to the present $Fe_{0.78}Tb_{0.05}B_{0.17}$ and $Fe_{0.73}Tb_{0.10}B_{0.17}$ samples for the values of magnetic moment from this simple model to be used in the analysis below. One further refinement is to reduce the saturation values of these moments (which will be used to analyse the 8 K data) to values appropriate to 300 K. These can be estimated using the reduced magnetization curves given in figure 5 in [8]. The $Fe_{0.78}Tb_{0.05}B_{0.17}$ sample has a Curie temperature close to 562 K, so that $T/T_C \approx 0.53$ at 300 K, and this gives a reduction of 19% in the moment values, while for the $Fe_{0.73}Tb_{0.10}B_{0.17}$, $T/T_C \approx 0.6$ at 300 K and the reduction is 24%. The magnetic moments predicted for the iron and terbium atoms in the two samples, at the two experimental temperatures, are given in table 2.

5. Non-spin-flip cross-sections

When a neutron passes through the sample and the direction of its spin is unchanged, the two non-spin-flip scattering cross-sections, $\frac{\partial\sigma^{++}}{\partial\Omega}$ and $\frac{\partial\sigma^{--}}{\partial\Omega}$, are given by

$$\frac{\partial\sigma^{\pm\pm}}{\partial\Omega} = \frac{\partial\sigma_{II}}{\partial\Omega} + \frac{1}{3}\frac{\partial\sigma_{NSI}}{\partial\Omega} + \left|\left\langle\sum_{ij}(b_i \mp d_i S_{zi})(b_j^* \mp d_j^* S_{zj}^*)\exp(iQ(r_i - r_j))\right\rangle\right|. \tag{3}$$

Table 2. The values of the collinear magnetic moments on the iron and terbium atoms in the two (Fe, Tb)B glasses are given, derived from the elemental values using the model described in section 3.

		Magnetic moment in μ_B	
Composition	Temperature (K)	μ_{Fe}	μ_{Tb}
$Fe_{0.78}Tb_{0.05}B_{0.17}$	300	1.60	6.81
	8	1.98	8.41
$Fe_{0.73}Tb_{0.10}B_{0.17}$	300	1.34	5.68
	8	1.76	7.47

The sign convention in equation (3) follows [10] and the term $\frac{\partial\sigma_{\mu}}{\partial\Omega}$ is the isotope incoherent cross-section which has the value 4.0×10^{-2} barns sr^{-1}/atom for both samples [13]. The third term includes both nuclear *and* magnetic neutron scattering. It depends on the sum, or the difference, of b_i the nuclear and $d_i S_i$ the magnetic scattering amplitudes of which the latter now depends on the *collinear components* S_z of the magnetic spins.

The double summation in equation (3) can be written in terms of the partial structure factors (PSFs) $S_{\alpha\beta}(Q)$ [14] of a metallic glass as shown by Blétry and Sadoc [15]:

$$\left|\left\langle\sum_{ij}(b_i \mp d_i S_{zi})(b_j^* \mp d_j^* S_{zj}^*)\exp(\mathrm{i}Q(r_i - r_j))\right\rangle\right| = \sum_{\alpha\beta} x_\alpha x_\beta (b_\alpha \mp p_\alpha(Q)(b_\beta \mp p_\beta(Q)))S_{\alpha\beta}(Q) + [\langle(b \mp p(Q))^2\rangle - \langle b \mp p(Q)\rangle^2]. \quad (4)$$

Here, the magnetic scattering amplitude is written as $p_i(Q)$ for brevity, and again depends only on S_z. The first term on the right-hand side of equation (4) is the total structure factor $S^{\pm\pm}(Q)$ defined in terms of the partial structure factors $S_{\alpha\beta}(Q)$, and the summation $\alpha\beta$ is over the atomic species present. The second term is the disorder scattering which arises from the presence of two or more different atoms in the sample (which will also have different values of magnetic moment). The two non-spin-flip cross-sections will have the same general form as the total structure factor $S(Q)$ of a metallic glass, each with a different amplitude which is also Q-dependent.

The non-spin-flip cross-sections for the $Fe_{0.78}Tb_{0.05}B_{0.17}$ glass measured at 300 and 8 K are shown in figures 1(b) and (c), respectively, and those for the $Fe_{0.73}Tb_{0.10}B_{0.17}$ sample in figures 2(b) and (c). Note that the vertical scale for non-spin-flip cross-sections is about 10 times greater than that used the spin-flip cross-sections. The non-spin-flip cross-sections of the $Fe_{0.78}Tb_{0.05}B_{0.17}$ glass at 300 K in figure 1(b) are 'conventional' in the sense that the first maximum in $S(Q)$ in the $\frac{\partial\sigma^{--}}{\partial\Omega}$ and $\frac{\partial\sigma^{++}}{\partial\Omega}$ channels coincide at the same value of $Q \approx 3.1$ Å^{-1}. This has been observed in all previous similar measurements on TM–met-based glasses [2–4, 16, 17] from the seminal work [15] onwards. However, the other three examples, $Fe_{0.78}Tb_{0.05}B_{0.17}$ at 300 K and $Fe_{0.73}Tb_{0.10}B_{0.17}$ at both 8 and 300 K, exhibit a hitherto unobserved shift of the first peak between the $\frac{\partial\sigma^{--}}{\partial\Omega}$ and $\frac{\partial\sigma^{++}}{\partial\Omega}$ channels, which can be most clearly seen in figures 1(c), 2(b) and (c).

6. Simulation of the non-spin-flip cross-sections of the (Fe, Tb)B glasses

These (Fe, Tb)B glasses are different from other TM–met-based glasses studied so far because the terbium atom is larger than any other substituted atom and it also carries a significantly larger

Table 3. The values of the nuclear scattering amplitudes b_i for iron, terbium and boron [13] are given together with the sums $(b_\alpha + p_\alpha(0))$ and differences $(b_\alpha - p_\alpha(0))$ of the nuclear and magnetic scattering amplitudes, in the forward limit where $f(Q) = 1$ when $Q = 0$.

Nuclear and magnetic scattering amplitudes in fm		
	$b_{Fe} = 9.54$ $b_{Tb} = 7.38$ $b_B = 5.30 - 0.213i$	
$Fe_{0.78}Tb_{0.05}B_{0.17}$		
$Q = 0$, $T = 300$ K	$p_{Fe}(0) = 0.268 \times 1.60 \times f(Q) = 4.29$	$b_{Fe} + p_{Fe}(0) = 13.83$
—	—	$b_{Fe} - p_{Fe}(0) = 5.25$
—	$P_{Tb}(0) = 0.268 \times 6.81 \times f(Q) = 18.25$	$b_{Tb} + p_{Tb}(0) = 25.63$
—	—	$b_{Tb} - p_{Tb}(0) = -10.87$
$Q = 0$, $T = 8$ K	$p_{Fe}(0) = 0.268 \times 1.98 \times f(Q) = 5.25$	$b_{Fe} + p_{Fe}(0) = 14.79$
—	—	$b_{Fe} - p_{Fe}(0) = 4.29$
—	$P_{Tb}(0) = 0.268 \times 8.41 \times f(Q) = 22.54$	$b_{Tb} + p_{Tb}(0) = 29.92$
—	—	$b_{Tb} - p_{Tb}(0) = -15.16$
	$P_B = 0$	
$Fe_{0.73}Tb_{0.10}B_{0.17}$		
$Q = 0$, $T = 300$ K	$p_{Fe}(0) = 0.268 \times 1.34 \times f(Q) = 3.59$	$b_{Fe} + p_{Fe}(0) = 13.13$
—	—	$b_{Fe} - p_{Fe}(0) = 5.95$
—	$P_{Tb}(0) = 0.268 \times 5.68 \times f(Q) = 15.22$	$b_{Tb} + p_{Tb}(0) = 22.60$
—	—	$b_{Tb} - p_{Tb}(0) = -7.84$
$Q = 0$, $T = 8$ K	$p_{Fe}(0) = 0.268 \times 1.76 \times f(Q) = 4.72$	$b_{Fe} + p_{Fe}(0) = 14.26$
—	—	$b_{Fe} - p_{Fe}(0) = 4.82$
—	$P_{Tb}(0) = 0.268 \times 7.47 \times f(Q) = 20.02$	$b_{Tb} + p_{Tb}(0) = 27.40$
—	—	$b_{Tb} - p_{Tb}(0) = -12.64$

magnetic moment. The nuclear scattering amplitudes b_i for iron, terbium and boron [13] are given in table 3 as well as the magnetic scattering amplitudes $p(Q)$ calculated (in the forward limit where $f(Q) = 1$ when $Q = 0$) from the magnetic moment values of table 2. There are, in fact, only six elements (and three isotopes) with values of b greater than 10 fm [13], but table 3 shows that the magnetic scattering amplitude of terbium *alone* is almost twice this in the forward limit. In addition, the sum $(b_{Tb} + p_{Tb}(0))$ and the difference $(b_{Tb} - p_{Tb}(0))$ are approximately 30 fm and −15 fm, respectively, using the saturation moment values. The negative value arises because a (++) neutron will 'see' a scattering amplitude $b_{Fe} - p_{Fe}(Q) \approx 4.82$ fm on each iron atom but $(b_{Tb} + p_{Tb}(Q)) \approx 27.40$ fm on each terbium atom, while a (−−) neutron will see scattering amplitudes of $b_{Fe} + p_{Fe}(Q) \approx 14.26$ fm and $(b_{Tb} - p_{Tb}(Q)) \approx -12.64$ fm respectively.

The shift of the first peak probably arises from the strong magnetic scattering from the terbium atoms, which will occur at smaller values of Q than the contributions from the iron atoms because of their larger size. Figures 2(a)–(d) support this suggestion, since the shift is greatest for the sample with the most terbium (10%), and greatest at low temperature, where the aligned S_z component of the terbium moment is largest.

This suggestion was tested by considering how the various atomic pair correlations will contribute to the non-spin-flip cross-sections. The characteristic values of $Q_{\alpha\beta} = 5/4(2\pi/r_{\alpha\beta})$ [18] which correspond to the known $r_{\alpha\beta}$ atomic pair distances were obtained from the Goldschmidt radii of iron and terbium and the tetrahedral covalent radius of boron, in the usual way [19]. The magnitude of each contribution was scaled to the weighting factor

Table 4. The weighting factors $\omega_{\alpha\beta}$ for the PSFs in $Fe_{0.73}Tb_{0.10}B_{0.17}$ glass at 8 K are given together with the characteristic $Q_{\alpha\beta}$-values for the corresponding atomic pair $r_{\alpha\beta}$ correlations, in increasing order downwards. (Goldschmidt radii: $r^{G}_{Fe} = 1.27$ Å, $r^{G}_{Tb} = 1.77$ Å; tetrahedral covalent radius: $r^{t}_{B} = 0.88$ Å.)

Atomic pair correlation	Interatomic distance (Å)	Corresponding Q value (Å^{-1})	Weighting factors $\omega_{\alpha\beta}$ for the PSFs in ferrimagnetic $Fe_{0.73}Tb_{0.10}B_{0.17}$ glass at $Q = 0$	
			$S^{--}(Q)$	$S^{++}(Q)$
Tb–Tb	$2r_{Tb} = 3.54$	2.22	0.016	0.146
Fe–Tb	$r_{Fe} + r_{Tb} = 3.04$	2.58	−0.261	0.376
Tb–B	$r_{Tb} + r_{B} = 2.65$	2.96	−0.023	0.096
Fe–Fe	$2r_{Fe} = 2.54$	3.09	1.074	0.242
Fe–B	$r_{Fe} + r_{B} = 2.15$	3.65	0.186	0.124
B–B	$2r_{B} = 1.76$	4.46	0.008	0.016

$\omega_{\alpha\beta}$ of the equivalent PSF,

$$S^{\pm\pm}(Q) = \omega^{\mp\mp}_{FeFe} S_{FeFe}(Q) + \omega^{\mp\mp}_{FeB} S_{FeB}(Q) + \omega^{\mp\mp}_{BB} S_{BB}(Q) + \omega^{\mp\mp}_{FeTb} S_{FeTb}(Q) + \omega^{\mp\mp}_{TbB} S_{TbB}(Q) + \omega^{\mp\mp}_{TbTb} S_{TbTb}(Q) \quad (5)$$

which depends on the concentration of the species and on their scattering amplitudes,

$$\begin{aligned} S^{\pm\pm}(Q) = {} & [(0.83 - x)^2 (b_{Fe} \mp p_{Fe}(Q))^2 S_{FeFe}(Q) \\ & + 2(0.83 - x)0.17(b_{Fe} \mp p_{Fe}(Q)) b_B S_{FeB}(Q) \\ & + (0.17)^2 b_B^2 S_{BB}(Q) + 2(0.83 - x)x(b_{Fe} \mp p_{Fe}(Q))(b_{Tb} \mp p_{Tb}(Q)) S_{FeTb}(Q) \\ & + 2x0.17(b_{Tb} \mp p_{Tb}(Q)) b_B S_{TbB}(Q) \\ & + x^2 (b_{Tb} \mp p_{Tb}(Q))^2 S_{TbTb}(Q)] / \langle b \mp p(Q) \rangle^2. \end{aligned} \quad (6)$$

Considering the $Fe_{0.73}Tb_{0.10}B_{0.17}$ glass with the proposed ferrimagnetic structure at 8 K and substituting into equation (6) from table 3 leads to the values of the $\omega_{\alpha\beta}$ which are shown in table 4.

The values given in this table indicate that $S^{--}(Q)$ is dominated by contributions for the $S_{FeFe}(Q)$, $S_{FeTb}(Q)$ and $S_{FeB}(Q)$ PSFs since the remaining three PSFs account for only 5% of the total. Its largest contribution from $S_{FeFe}(Q)$ ($\omega_{FeFe} = 1.074$) will peak at $Q_{FeFe} \approx 3.1$ Å^{-1}. But the second largest contribution from $S_{FeTb}(Q)$ at $Q_{FeTb} \approx 2.58$ Å^{-1} has a negative ω_{FeTb} and this will produce a sharp leading edge to the first peak in $S^{--}(Q)$. In contrast, $S^{++}(Q)$ has significant contributions from five of the six PSFs and only $S_{BB}(Q)$ is negligible ($\omega_{BB} = 0.0161$). More important, positive contributions from $S_{TbTb}(Q)$ and $S_{FeTb}(Q)$ occur at the smaller values of $Q_{TbTb} \approx 2.2$ Å^{-1} and $Q_{FeTb} \approx 2.6$ Å^{-1}, respectively, so that the first maximum in $S^{++}(Q)$ will be shifted to smaller Q-values than the first maximum in $S^{--}(Q)$ in agreement with the observations.

It seemed worthwhile to extend these calculations and make a more complete simulation of the measured non-spin-flip cross-sections. There appear to be no examples in the literature where the six PSFs of (Fe, RE)B-type glasses have been derived; however, the three PSFs have been obtained for the binary glass $Fe_{80}B_{20}$ from a combination of x-ray and neutron diffraction experiments with isotope-substituted samples [20]. The $S_{FeFe}(Q)$ and $S_{FeB}(Q)$ PSFs were digitized from figure 5 of [20] using the package *g3data* [25] over a range 0.5 Å^{-1} < Q < 8.0 Å^{-1} with approximately 200 data points. They are shown in the upper part of figure 4. The $S_{BB}(Q)$ PSF was not required in the present simulations. These PSFs

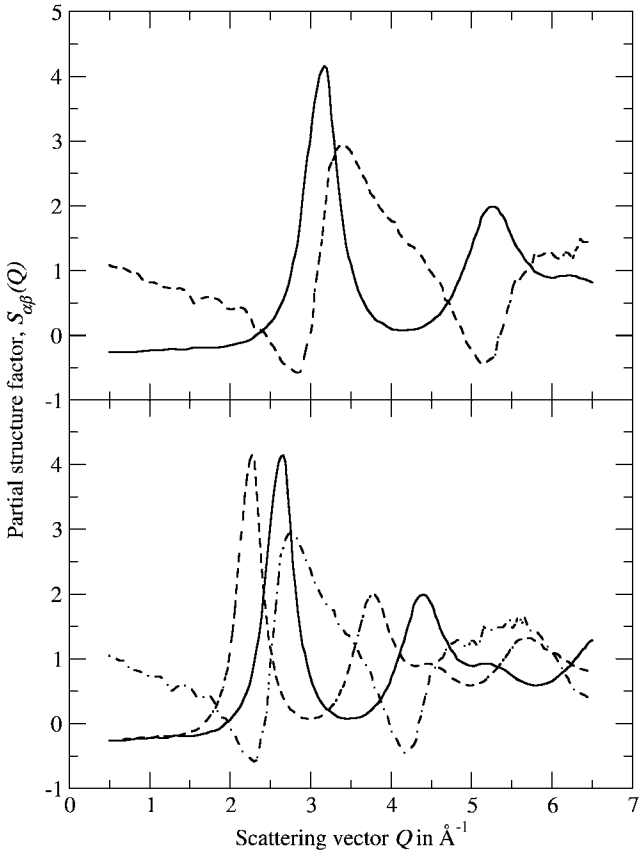

Figure 4. The partial structure factors $S_{\mathrm{FeFe}}(Q)$ (solid line) and $S_{\mathrm{FeB}}(Q)$ (dashed line) measured for $Fe_{80}B_{20}$ glass [20] are shown in the top diagram. In the lower diagram approximations to the $S_{\mathrm{TbTb}}(Q)$ (dashed line), $S_{\mathrm{FeTb}}(Q)$ (solid line) and $S_{\mathrm{TbB}}(Q)$ (dash–dot line) partial structure factors are shown, derived by scaling the scattering vector Q according to the inverse ratios of the interatomic pair distances $r_{\alpha\beta}$.

were then used to generate *approximations* to the three absent PSFs $S_{\mathrm{TbTb}}(Q)$, $S_{\mathrm{FeTb}}(Q)$ and $S_{\mathrm{TbB}}(Q)$ by scaling their Q-axes by the factors $r_{\mathrm{Fe}}/r_{\mathrm{Tb}} = 0.718$, $r_{\mathrm{Fe}}/\langle r_{\mathrm{Fe}} + r_{\mathrm{Tb}}\rangle = 0.836$ and $\langle r_{\mathrm{Fe}} + r_{\mathrm{B}}\rangle/\langle r_{\mathrm{Tb}} + r_{\mathrm{B}}\rangle = 0.811$, respectively. The rescaled curves were then interpolated to give data points at the same values of Q as the two original PSFs and are shown in the lower part of figure 4.

Although this scaling process appears to be very arbitrary, its main justification is that it turns out to be surprisingly successful, as will be shown below. This kind of scaling has often been used in the past in the search for a 'universal structure prototype' for metallic glasses. The possibility of finding structural prototypes for the TM–met glasses in their stable crystalline phases has been considered by several different groups; see for example [21, 22]. This even led to the radical suggestion that *one set* of three partial pair correlation functions alone might be sufficient to describe the structures of *all* binary metallic glasses [23, 24]. In fact, remarkable agreement has been found between experiment and calculation for a wide variety of glasses using this approach. Generally, scaling PSFs or the atomic pair density functions is likely to be most successful when (as here) there is no reason to believe that the Fe–Tb substitution is

other than random and the terbium concentration relatively low. This means that the dominant influence of the substitution is to cause an overall expansion of the parent glassy structure.

Simulations were therefore made of the $\frac{\partial\sigma^{--}}{\partial\Omega}$ and $\frac{\partial\sigma^{++}}{\partial\Omega}$ cross-sections at both temperatures of 8 and 330 K and for both the $Fe_{0.78}Tb_{0.05}B_{0.17}$ and $Fe_{0.73}Tb_{0.10}B_{0.17}$ glasses, by direct substitution into equations (3), (4) and (6). The nuclear b and $p(Q)$ magnetic scattering amplitudes were taken from table 3; the form factor $f(Q)$ dependence was introduced using the seven parameter fits for the Fe^{3+} and Er^{+} ions specified in [26], and the PSFs used were those in figure 4. The diffuse scattering term in equation (4) was calculated and added to the total cross-sections, but the two incoherent contributions in equation (3) were neglected as being too small to influence the outcome of the simulation.

The cross-sections calculated initially had the correct characteristics, but were not a good match to the data, which was attributed to their Q resolution. A polarized beam spectrometer such as IN20 needs a more open collimation (to ensure high enough count rates in the four spin-dependent channels) than a diffractometer used for measuring the $S(Q)$s of metallic glasses. The calculated non-spin-flip cross-sections were therefore convoluted with a Gaussian whose half-width was systematically increased until the calculated features matched those of the measured cross-sections. The final simulations are shown in figures 1(b), (c), 2(b) and (c), where the dotted line represents the $\frac{\partial\sigma^{--}}{\partial\Omega}$ and the solid line the $\frac{\partial\sigma^{++}}{\partial\Omega}$ cross-sections, respectively. The level of agreement is most satisfactory. In particular, the profile of the first peak in $\frac{\partial\sigma^{--}}{\partial\Omega}$ is very well reproduced. The considerable difference in both the magnitude and the position of the first peaks in $\frac{\partial\sigma^{--}}{\partial\Omega}$ and $\frac{\partial\sigma^{++}}{\partial\Omega}$ is faithfully simulated in every case. The agreement is probably best for the $Fe_{0.78}Tb_{0.05}B_{0.17}$ sample, where the statistical variations are smaller. There are increases in the measured cross-sections at the smallest values of Q, which are not well reproduced in the simulation, especially for the $Fe_{0.73}Tb_{0.10}B_{0.17}$ sample. This may be a real effect, such as an increase in magnetic scattering at small Q-values caused by magnetic correlations on longer length scales, which are not in the model. The effect is probably enhanced by a limitation of the convolution because the full width of the Gaussian does not overlap with the data points at either end of the Q range.

In general, these simulations are in good agreement with the data and provide excellent support for the explanation of the shift of the first peak between the $\frac{\partial\sigma^{--}}{\partial\Omega}$ and $\frac{\partial\sigma^{++}}{\partial\Omega}$ cross-sections proposed above. Their success provides support for the derivation of the absent PSFs $S_{TbTb}(Q)$, $S_{FeTb}(Q)$ and $S_{TbB}(Q)$ by scaling, which was discussed above.

7. Conclusions

A search for non-collinear ferromagnetism in terbium-substituted $(Fe_{0.83-x}Tb_x)B_{0.17}$ metallic glasses has been made by polarized beam neutron scattering, prompted by reports of a 'random anisotropy phase' at low temperatures.

The spin-flip cross-sections $\frac{\partial\sigma^{\pm\mp}}{\partial\Omega}$ were found to be

(i) small,
(ii) independent of the scattering vector Q,
(iii) independent of the temperature, and
(iv) of the same magnitude as the nuclear incoherent cross-section.

This means that the magnetic structures in these glasses are almost certainly collinear. A simple model for the collinear ferrimagnetic state has therefore been presented in which the magnetic moments on the terbium atoms ($\mu_{Tb} = 9.34\ \mu_B$) are aligned antiparallel to those on the iron atoms ($\mu_{Fe} = 2.2\ \mu_B$) and both reduce to zero by $x = 0.50$ in agreement with magnetization data. The non-spin-flip cross-sections were found to show a hitherto unobserved shift of the

first peak between the $\frac{\partial\sigma^{--}}{\partial\Omega}$ and $\frac{\partial\sigma^{++}}{\partial\Omega}$ cross-sections. Simulations were made of these cross-sections starting from the collinear ferrimagnetic model, using measured and derived partial structure factors. The simulations correctly predicted the magnitude of the shift of the first peaks in all four measured data sets. This behaviour is attributed to

(i) the collinear ferrimagnetic correlations between the magnetic moments,
(ii) the very strong magnetic scattering from the terbium atoms, and
(iii) the fact that the terbium atoms are large, so that the contributions to the total scattering from first neighbour terbium atoms occur at smaller Q-values than those from the other pair correlations present.

Acknowledgments

The neutron experiments were made within the EPSRC Neutron Beam Programme and the help of the staff at the Institut Laue-Langevin is gratefully acknowledged. The authors would also like to thank Mr J Newell for his assistance in the sample preparation.

References

[1] Mizoguchi T 1978 *Sci. Rep. RITU Suppl.* A 117
[2] Cowley R A, Patterson C, Cowlam N, Ivison P K, Martinez J and Cussen L D 1991 *J. Phys.: Condens. Matter* **3** 9521
[3] Wildes A R, Cowley R A, Al-Heniti S, Cowlam N, Kulda J and Lelièvre-Berna E 1998 *J. Phys.: Condens. Matter* **10** 2716
[4] Wildes A R, Stewart J R, Cowlam N, Al-Heniti S, Kiss L F and Kémeny T 2003 *J. Phys.: Condens. Matter* **15** 675
[5] Paulose P L, Nagaragan R, Nagarajan V and Vijayarahavan R 1986 *J. Magn. Magn. Mater.* **54–57** 257–8
[6] Harris R, Plischke M and Zuckermann M J 1973 *Phys. Rev. Lett.* **31** 160–2
[7] Greenhough R D, Gregory T J, Clegg S J and Purdey J H 1991 *J. Appl. Phys.* **70** 6534–6
[8] Greenhough R D, Gregory T J and Purdey J H 1991 *J. Appl. Phys.* **70** 6534–6
[9] Cowlam N and Carr G E 1985 *J. Phys. F: Met. Phys.* **15** 1109
[10] Moon R M, Riste T and Koehler W C 1969 *Phys. Rev.* **181** 920
[11] Cowlam N and Wildes A R 2003 *J. Phys.: Condens. Matter* **15** 521
[12] Wildes A R 1999 *Rev. Sci. Instrum.* **70** 4241
[13] Sears V F 1992 *Neutron News* **3** 26
[14] Faber T E and Ziman J M 1964 *Phil. Mag.* **11** 153
[15] Blétry J and Sadoc J F 1975 *J. Phys. F: Met. Phys.* **5** L111
[16] Dubois J M, Chiex P, Le Caer G, Schweitzer J and Blétry J 1982 *Nucl. Instrum. Methods* **199** 315
[17] Guoan Wu, Cowlam N, Davies H A, Cowley R A, McK Paul D and Stirling W G 1982 *J. Physique Coll.* **43** C7 71
[18] Klug H P and Alexander L E 1974 *X-ray Diffraction Procedures* (New York: Wiley)
[19] Cargill G S III 1975 *Solid State Phys.* **30** 227
[20] Nold E, Lamparter P, Olbrich H, Rainer-Harbach G and Steeb S 1981 *Z. Naturf.* a **36** 1032
[21] Faigel G, de Vries W H, Jansen H J F, Tegze M and Vincze I 1980 *Metallic Glasses Science and Technology* vol 1, ed C Hargitai, I Bakonyi and T Kemény (Budapest: R.I.S.S.P.) p 275
[22] Aur S, Egami T and Vincze I 1982 *Proc. 4th Int. Conf. Rapidly Quen Met.* vol 1, ed T Masumoto and K Suzuki (Sendai: Jap Inst Met) p 351
[23] Siltsma J and Thijsse B 1988 *J. Non-Cryst. Solids* **101** 135
[24] Siltsma J and Thijsse B 1991 *J. Non-Cryst. Solids* **135** 146
[25] http://www.acclab.helsinki.fi/~frantz/software/g3data.php
[26] Brown P J 1995 *International Tables for Crystallography* vol C, ed A J C Wilson (Dordrecht: Kluwer) p 391